



OPEN ACCESS

EDITED BY

Pengfei Xu,
University of Pittsburgh, United States

REVIEWED BY

Zhengping Huang,
Guangdong Second Provincial General
Hospital, China
Amy J. Naylor,
University of Birmingham, United Kingdom

*CORRESPONDENCE

Edward M. Schwarz
✉ Edward_Schwarz@
URMC.Rochester.edu

RECEIVED 10 August 2023

ACCEPTED 20 November 2023

PUBLISHED 14 December 2023

CITATION

Peng Y, Kenney HM, de Mesy Bentley KL,
Xing L, Ritchlin CT and Schwarz EM (2023)
Distinct mast cell subpopulations within
and around lymphatic vessels regulate
lymph flow and progression of
inflammatory-erosive arthritis in
TNF-transgenic mice.
Front. Immunol. 14:1275871.
doi: 10.3389/fimmu.2023.1275871

COPYRIGHT

© 2023 Peng, Kenney, de Mesy Bentley,
Xing, Ritchlin and Schwarz. This is an open-
access article distributed under the terms of
the [Creative Commons Attribution License
\(CC BY\)](https://creativecommons.org/licenses/by/4.0/). The use, distribution or
reproduction in other forums is permitted,
provided the original author(s) and the
copyright owner(s) are credited and that
the original publication in this journal is
cited, in accordance with accepted
academic practice. No use, distribution or
reproduction is permitted which does not
comply with these terms.

Distinct mast cell subpopulations within and around lymphatic vessels regulate lymph flow and progression of inflammatory-erosive arthritis in TNF-transgenic mice

Yue Peng^{1,2}, H. Mark Kenney^{1,2}, Karen L. de Mesy Bentley^{1,2},
Lianping Xing^{1,2}, Christopher T. Ritchlin^{1,3}
and Edward M. Schwarz^{1,2*}

¹Center for Musculoskeletal Research, University of Rochester Medical Center, Rochester, NY, United States, ²Department of Pathology & Laboratory Medicine, University of Rochester Medical Center, Rochester, NY, United States, ³Department of Medicine, Division of Allergy, Immunology, Rheumatology, University of Rochester Medical Center, Rochester, NY, United States

Objective: Inflammatory-erosive arthritis is exacerbated by dysfunction of joint-draining popliteal lymphatic vessels (PLVs). Synovial mast cells are known to be pro-inflammatory in rheumatoid arthritis (RA). In other settings they have anti-inflammatory and tissue reparative effects. Herein, we elucidate the role of mast cells on PLV function and inflammatory-erosive arthritis in tumor necrosis factor transgenic (TNF-tg) mice that exhibit defects in PLVs commensurate with disease progression.

Methods: Whole mount immunofluorescent microscopy, toluidine blue stained histology, scanning electron microscopy, and *in silico* bioinformatics were performed to phenotype and quantify PLV mast cells. Ankle bone volumes were assessed by μ CT, while corresponding histology quantified synovitis and osteoclasts. Near-infrared indocyanine green imaging measured lymphatic clearance as an outcome of PLV draining function. Effects of genetic MC depletion were assessed via comparison of 4.5-month-old WT, TNF-tg, MC deficient *Kit^{W-sh/W-sh} (cKit^{-/-})*, and TNF-tg x *cKit^{-/-}* mice. Pharmacological inhibition of mast cells was assessed by treating TNF-tg mice with placebo or cromolyn sodium (3.15mg/kg/day) for 3-weeks.

Results: PLVs are surrounded by MCT⁺/MCPT1⁺/MCPT4⁺ mast cells whose numbers are increased 2.8-fold in TNF-tg mice. The percentage of perivascular degranulating mast cells was inversely correlated with ICG clearance. A population of MCT⁺/MCPT1⁻/MCPT4⁻ mast cells were embedded within the PLV structure. *In silico* single-cell RNA-seq (scRNAseq) analyses identified a population of PLV-associated mast cells (marker genes: *Mcpt4*, *Cma1*, *Cpa3*, *Tpsb2*, *Kit*, *Fcer1a* & *Gata2*) with enhanced TGF β -related signaling that are phenotypically distinct from known MC subsets in the *Mouse Cell Atlas*. *cKit^{-/-}* mice have greater lymphatic defects than TNF-tg mice with exacerbation of

lymphatic dysfunction and inflammatory-erosive arthritis in TNF-tg x cKit^{-/-} vs. TNF-Tg mice. Cromolyn sodium therapy stabilized PLV mast cells, increased TNF-induced bone loss, synovitis, and osteoclasts, and decreased ICG clearance.

Conclusions: Mast cells are required for normal lymphatic function. Genetic ablation and pharmacological inhibition of mast cells exacerbates TNF-induced inflammatory-erosive arthritis with decreased lymphatic clearance. Together, these findings support an inflammatory role of activated/degranulated peri-PLV mast cells during arthritic progression, and a homeostatic role of intra-PLV mast cells, in which loss of the latter dominantly exacerbates arthritis secondary to defects in joint-draining lymphatics, warranting investigation into specific cellular mechanisms.

KEYWORDS

T32GM007356, F30AG076326, R01AG059775, R01AR069000, R01AR056702, mast cell, lymphatic vessel, inflammatory-erosive arthritis

Introduction

Rheumatoid arthritis (RA) is a chronic inflammatory joint disease that affects up to 1% of the population worldwide (1). Besides pannus tissue invasion, cartilage degradation and focal bone erosion of joints, RA patients show altered lymphatic function, as evidenced by reduced lymphatic vessel contraction and slower lymphatic clearance rate compared to healthy controls (2–4). Three distinct mechanisms underlie lymphatic dysfunction in murine models of RA. First, loss of lymphatic vessel contractions is observed over the course of progressive arthritis secondary to extensive tissue damage in the setting of chronic inflammation (5). Second, accumulation and translocation of B cells to the sinuses obstructs passive lymphatic flow in joint draining lymph nodes (6, 7). Finally, release of local vasodilators, such as nitric oxide, likely generated by peri-lymphatic inflammatory cells that express inducible-nitric oxide synthase, contribute to reduced lymphatic flow (8, 9).

In RA patients, mast cells are also present throughout the RA synovial sublining, with occasional microanatomic clustering in the pannus near sites of cartilage and bone erosion, and comprise 5% or more of the expanded synovial cell population (10–12). Synovial mast cells produce cytokines (i.e. TNF, IL-1 and IL-6) that mediate monocyte/macrophage recruitment, differentiation, and activation, and serve as targets of RA biologic therapies (13–15). Additionally, some mast cells promote long term effects in joint tissues through the recruitment of inflammatory cells and activation of stromal cells resulting in fibrosis and accelerated angiogenesis (15, 16). The number of accumulated mast cells differs substantially from

patient to patient and this variation is associated with the intensity of joint inflammation (17). In fact, the presence of mast cells in early RA synovial tissue correlates with disease severity and supports B cell autoantibody production (18). Thus, evidence from preclinical and clinical studies support both a pro-inflammatory and catabolic role for mast cells in RA (19).

Mast cells have also been described as tissue resident, including lymphatics. The literature describes two subtypes of mast cells: mucosal mast cells that produce tryptase and connective tissue mast cells that produce chymase, tryptase, and carboxypeptidases (20). Mast cells are recognized as potent regulators of lymphatic vessel function based on their anatomical proximity and ability to produce, store, and release various inflammatory and vasoactive mediators (21–23). Mast cells release mediators (e.g., histamine) that impact the contractility of lymphatic vessels (21, 23, 24), which is critical for efficient drainage of joint inflammation. Histamine (H) 1 receptors enhance and H2 receptors slow down lymphatic contractions, the dominant effect being an increased contractile activity (24).

The role of mast cell regulation of joint draining lymphatics and their functions in RA remains undefined. To identify the effector cells that control lymphatic vessel contractions efferent to inflamed joints in RA, we performed exploratory whole mount immunofluorescent microscopy (WMIFM) on popliteal lymphatic vessels (PLVs) from tumor necrosis factor-transgenic (TNF-tg) mice with inflammatory-erosive arthritis (25) and their wild-type (WT) littermates. Through this investigation, we serendipitously observed a population of peri-PLV cells that bind fluorescently-conjugated isotype control antibodies with the histologic appearance of mast cells (Supplementary Figure 1). Moreover, numbers of these proposed peri-PLV mast cells were markedly increased around the lymphatic vessels of TNF-tg mice. Based on these observations and the open questions about the role of peri-PLV mast cells on lymphatic function and association with RA pathogenesis, we hypothesized that: i) peri-PLV cells are indeed

Abbreviations: LMC, lymphatic muscle cell; PLV, Popliteal Lymphatic Vessels; TBFG, Toluidine Blue and Fast Green; WMIF, Whole mount immunofluorescent; WMIFM, Whole mount immunofluorescent microscopy; MCPT, Mast Cell Protease; MCT, Mast Cell Tryptase; SEM, Scanning Electron Microscopy.

pro-inflammatory mast cells that regulate lymphatic function by releasing (degranulating) catabolic factors, and ii) genetic ablation and pharmacological inhibition of mast cells ameliorates lymphatic dysfunction and reduces inflammatory-erosive arthritis in TNF-tg mice.

Materials and methods

Mouse models

All animal research was conducted with approval by the University of Rochester Institutional Animal Care and Use Committee. TNF-tg mice (3647 line) (25) were initially acquired from Dr. George Kollias and have since been maintained at the University of Rochester. The TNF-tg mice were bred as heterozygotes, and WT littermates were used as controls (C57BL/6 genetic background). B6.Cg-*Kit*^{W-sh}/HNihrJaeBsmJ (*Kit*^{W-sh/W-sh} or *cKit*^{-/-}) mice were purchased from The Jackson Laboratory (Bar Harbor, ME, Strain #:030764) and maintained at the University of Rochester vivarium. For crossing between the two strains, TNF-tg or TNF-tg x *cKit*^{+/-} mice were used as male breeders, and *cKit*^{-/-} mice as female breeders. For all *in vivo* longitudinal outcome measures, 4 to 5-month-old male mice were anesthetized with 1–3% isoflurane. All mice were euthanized with a lethal dose of ketamine/xylazine cocktail (intraperitoneal) followed by cervical dislocation. A total of 14 mice were used in this study, with a minimum of $n = 3$ experimental units evaluated for each group ($n=8$ for WT, $n=4$ for *cKit*^{-/-}, $n=4$ for TNF-tg, $n=3$ for TNF-tg x *cKit*^{-/-}). Out of the total 8 WT animals, 3 WT mice received all examinations. The remaining 5 WT mice underwent microCT and histologic assessment, as they served as controls for their same-age double transgenic mice, which unfortunately died before the dissection.

Whole mount immunofluorescent microscopy

PLVs were harvested and fixed as previous described (4, 26). Briefly, fixed PLVs were blocked with 5% normal goat serum (NGS; ThermoFisher Scientific Cat# 50062Z)/1 × TBS/0.3% Triton X-100 (BioRad, Cat# 1706435) for 1 h at room temperature (RT), and then incubated with the primary antibodies diluted in 5% NGS/1 × TBS/0.3% Triton X-100 overnight at 4°C. For α SMA labeling, we utilized mouse anti- α SMA antibodies (AlexaFluor 488 conjugate; ThermoFisher Scientific Cat# 53-9760-82, 1:100 dilution). Primary conjugated isotype control staining was performed with mouse IgG2b antibodies (AlexaFluor 555; ThermoFisher Scientific Cat# A-21428, 1:100 dilution).

To validate the mast cell subtypes, the following primary antibodies were used in this study: Rabbit anti-human Mast Cell Tryptase IgG (mouse reactivity; Bioss Antibodies Cat# BSM-52533R; 1:100 dilution); Rat anti-mouse Mcpt-1 IgG1 (ThermoFisher Scientific Cat# 14-5503-80; 1:20 dilution); Goat anti-Mouse Mcpt-4 Polyclonal (ThermoFisher Scientific Cat#

PA5-142454; 1:100 dilution); Rabbit anti-human CMA1(Mcpt-5) IgG (mouse reactivity; ThermoFisher Scientific Cat# PA5-79053; 1:50 dilution); Rabbit anti-mouse Chymase antibody (Abcam Cat# ab233103; 1:50 dilution). To prevent non-specific labeling of Fc receptors (FcR), exclusively secondary antibodies below featuring F(ab) fragments were utilized: Anti-rabbit IgG (H+L), F(ab')₂ Fragment (Alexa Fluor 555 Conjugate; Cell Signaling Technology Cat# 4413; 1:1000 dilution); F(ab')₂ Donkey anti-Rat IgG ((Alexa Fluor 647 Conjugate; Jackson ImmunoResearch Inc Cat#712-606-153; 1:1000 dilution); F(ab')₂ Rabbit anti-Goat IgG (Alexa Fluor 647 Conjugate; Jackson ImmunoResearch Inc Cat# 305-606-006; 1:500 dilution). After 3 × 10 min washes in 1 × TBS/0.1% Triton X-100 following antibody incubation, the PLVs were mounted on a microscope slide with one drop of both ProLong Gold Antifade Mountant (ThermoFisher Scientific Cat# P36930) and NucBlue Live ReadyProbes Reagent (Hoechst 33342 formulation; ThermoFisher Scientific Cat# R37605). The PLVs were then imaged using a VS120 Slide Scanner for α SMA coverage analysis as previously described (4, 26).

Histochemistry

For histochemistry of mast cells, PLVs were subjected to two different preprocessing approaches for further toluidine blue and fast green (TBFG) staining. One group of PLVs was paraffin-embedded and longitudinally sectioned. Another group of PLVs had the coverslip carefully removed to enable whole mount TBFG staining after processing for WMIFM imaging in order to preserve the tissue at its original location and morphology for direct comparison. For sectioned PLVs, the sections underwent deparaffinization and hydration to distilled water, while the whole mounted PLVs were washed with distilled water. For TBFG staining, the tissue was exposed to 0.5% potassium permanganate for 2 minutes, followed by 1% potassium metabisulfite for 1 minute and rinsing with running tap water for 3 minutes. Subsequently, the tissue was stained with 0.02% toluidine blue for 5 minutes and 0.08% fast green for 30 seconds. Distilled water was used for a 30-second rinse between each staining procedure. Finally, the slides were dehydrated, mounted, and mast cells quantified.

For histochemistry of ankles and quantification of synovitis and osteoclasts, lower limbs of the mice were processed for paraffin embedded and demineralized hematoxylin and eosin (H&E; synovium) or tartrate-resistant acid phosphatase (TRAP; osteoclasts) histology, as previously described (9). All slides were scanned with an Olympus VS120 (full slide scans available upon request), and quantitative histomorphometry for synovial and TRAP⁺ tissue area was performed with Visiopharm (Hoersholm, Denmark, version 2021.04.0.10211), as previously described (4).

Scanning electron microscopy

SEM was performed, as previously described (4). Briefly, PLVs were fixed in 4% paraformaldehyde/2.5% glutaraldehyde/0.1M cacodylate overnight, post-fixed in buffered 1% osmium tetroxide,

dehydrated, critically point dried, mounted onto aluminum stubs and sputtercoated with gold prior to imaging using a Zeiss Auriga FE SEM. Three SEM micrographs per sample group were randomly chosen for descriptive analysis.

Near infrared-indocyanine imaging and quantification of lymphatic function

The subcutaneous injection of 10 μ l of a 0.1 mg/ml ICG solution in water was administered to both hind footpads of the mouse. The fluorescence of the footpad was measured in an IVIS Live Animal Imaging System (Caliper Life Sciences Inc.) one hour after injection (baseline) to capture the maximum fluorescence signal intensity, and again at six hours to quantify the remaining fluorescence, where the difference between these timepoints represents lymphatic clearance. Thus, the ratio of the fluorescence difference and baseline fluorescence was used to quantify lymphatic clearance as a biomarker of PLV function and drainage from the footpad.

Micro-CT quantification of talus bone volume

Semiautomated quantification of talus bone volume was performed, as previously described (4). Briefly, micro-CT hindpaw datasets were acquired using a VivaCT 40 (Scanco Medical, Bassersdorf, Switzerland), and all *in vivo* scans were collected with the following imaging parameters: 55 kV, 145 μ A, 300 ms integration time, 2048 \times 2048 pixels, 1000 projections over 180°, resolution 17.5 μ m isotropic voxels. Image collection for the hindpaws was completed in 30-45 min. Semiautomated 3D rendering of the ankle bones with volumetric quantification of the talus bone was performed with Amira software (ThermoFisher Scientific, version 4.6.0).

Cromolyn sodium treatment

Ten 4-month-old female TNF-Tg mice received baseline micro-CT and near-infrared indocyanine green scans to determine ankle bone volume and lymphatic clearance, respectively, and randomized to 3-weeks of daily intraperitoneal injections of placebo (PBS) or cromolyn sodium (CS) (3.15 mg/kg), as previously described (27). All mice were included in the study, except for one CS-treated animal, which was excluded from histologic assessment due to post-measurement mortality. Otherwise, no mice or samples were excluded from the study.

Bioinformatic single-cell RNA-sequencing analysis

To evaluate PLV-associated mast cells and other mast cell subtypes, we performed further bioinformatic analysis using our published single-cell RNA-sequencing (scRNAseq) dataset of PLVs (GSE190999,(28)) compared to a publicly available single-cell

transcriptomics *Mouse Cell Atlas* (29–31). Analysis was performed in R (v4.1.2) with clustering and differential gene expression analysis performed in Seurat (v4.3.0), as previously described (28). The differentially expressed genes (\log_2 fold-change < or >1, FDR<0.05) were then input into WikiPathway and Elsevier pathway analyses.

Statistics

We performed statistical analyses using GraphPad Prism (v9.1.1; Boston, MA, USA) to assess the significance of the observed differences. All statistical tests were two-tailed, and a p-value of less than 0.05 was considered statistically significant. Unpaired t-test was used in quantification of the MCT⁺ cells and FcR^{high} peri-PLV cells between WT and TNF-tg animals; and all comparison of WT, cKit^{-/-}, TNF-tg and TNF-tg x cKit^{-/-} animals; and all comparison between CS treated or saline treated TNF-tg animals. Additionally, we employed linear regression analysis to examine inter-user reliability of determining non-degranulating mast cells vs degranulating mast cells, regression of ICG clearance % vs. % degranulating mast cells in TNF-tg mice, and the association between of % degranulating mast cells vs. age. The results were reported as simple linear regressions with R² and p-value.

Results

Demonstration of increased peri-PLV mast cells in TNF-Tg mice with inflammatory arthritis

To verify the identity of the peri-PLV FcR^{high} population as mast cells, we performed WMIFM on PLVs from WT, TNF-tg, and mast cell deficient cKit^{-/-} mice with primary antibodies against mast cell tryptase (MCT) and fluorescent secondary Fab, and then reimaged the PLV after histochemical staining for TBFG (Figures 1A–C). Consistent with our hypothesis, we observed MCT⁺ cells that also stained purple from the TBFG (indicating the presence of heparin and histamine within their granules (32)) around WT PLVs whose numbers were 2.8-fold increased around TNF-tg PLV (Figure 1D; WT: 16.41 \pm 6.269; TNF-tg: 39.86 \pm 12.93; p=0.0005), and were completely absent in tissue from cKit^{-/-} mice. To further validate the identity of these peri-PLV cells, we performed scanning electron microscopy, which demonstrated phenotypic pancake-shaped mast cells that were distributed around the connective tissue surrounding the PLV (Figures 1E, F, red arrows). Based on these results, we conclude that the expanded peri-PLV cells in TNF-tg mice are indeed mast cells.

Degranulating peri-PLV mast cells negatively correlate with PLV function in WT and TNF-tg mice

Scrutiny of the TBFG-stained PLV histology sections revealed that WT mast cells appear to be stable (Figure 2A), while most TNF-tg

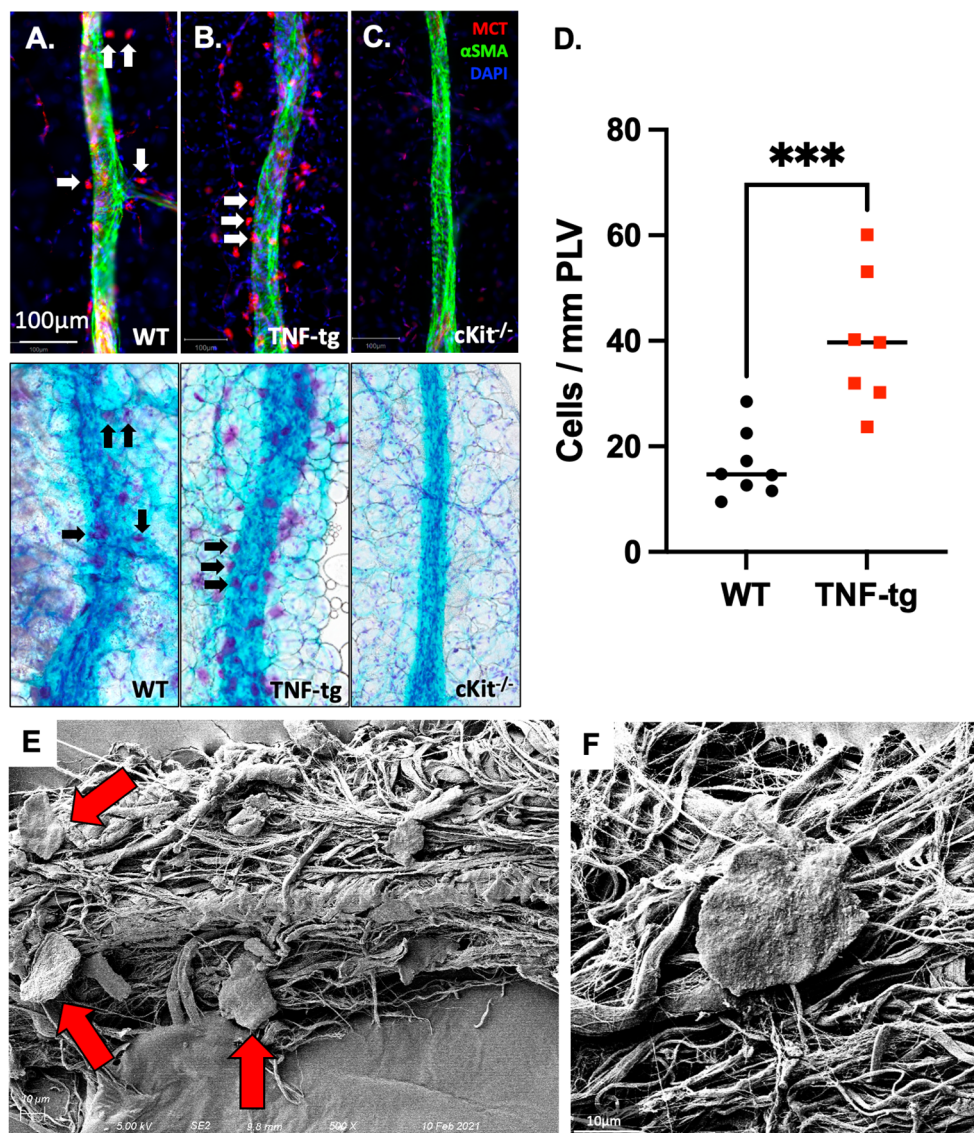


FIGURE 1 Mast cells accumulate around PLVs in TNF-tg mice with inflammatory arthritis. PLVs were harvested and processed for WMIF microscopy at 20x for α SMA (green) and mast cell tryptase (MCT, red). Subsequently, the same tissue underwent TBFG staining for light microscopy. Representative images are shown for WT (A), TNF-tg (B), and cKit^{-/-} (C) PLV. Note that the MCT⁺ cells (white arrows) are also toluidine blue stained (black arrows). The number of peri-lymphatic MCT⁺ cells per mm of WT and TNF-Tg PLV (n=8) was quantified, and data for each PLN are presented with the mean \pm SD (D, ***p < 0.001 via unpaired t-test). Scanning electron microscopy (SEM) was performed on WT PLVs with attached peri-lymphatic tissue, and representative images obtained at x500 (E) and x5,000 (F) are shown highlighting mast cells with their typical pancake-shape (red arrows).

mast cells appeared to be degranulated with unclear cellular borders and large cytoplasmic vesicles (Figure 2B). To validate these distinct non-degranulating vs. degranulating mast cell phenotypes, two independent observers (YP & HMK) performed double-blinded histomorphometric analysis, which produced excellent inter-user reliability results (Figure 2C; R² = 0.9654, p < 0.0001, ICC = 0.973). Given that mast cells are known to release histamine and proinflammatory cytokines that impact the contractility of lymphatic muscle cells (LMCs) (21, 23), we hypothesized that release of proinflammatory mediators by peri-PLV mast cells via degranulation may contribute to PLV dysfunction during the progress of inflammatory-erosive arthritis. To test this, we quantified PLV draining function in both WT and TNF-tg mice using near-infrared

indocyanine green imaging, after which we harvested the PLVs to quantify mast cell degranulation via TBFG stained histomorphometry. As predicted, we observed a robust negative correlation between the percentage of degranulating peri-vascular mast cells and the ICG clearance function of PLVs (Figure 2D; R² = 0.6711; p=0.0461). Of note is that the percentage of degranulating peri-PLV mast cells was not associated with age of the TNF-tg mice (Supplementary Figure 2), suggesting that this mast cell phenotype is primarily the result of TNF exposure in these mice independent of the chronicity of the inflammation. Together, these results demonstrate that TNF-tg mice exhibit both increased number and degranulation of peri-PLV mast cells, potentially releasing histamine and other effector molecules that might impact joint-draining lymphatic function.

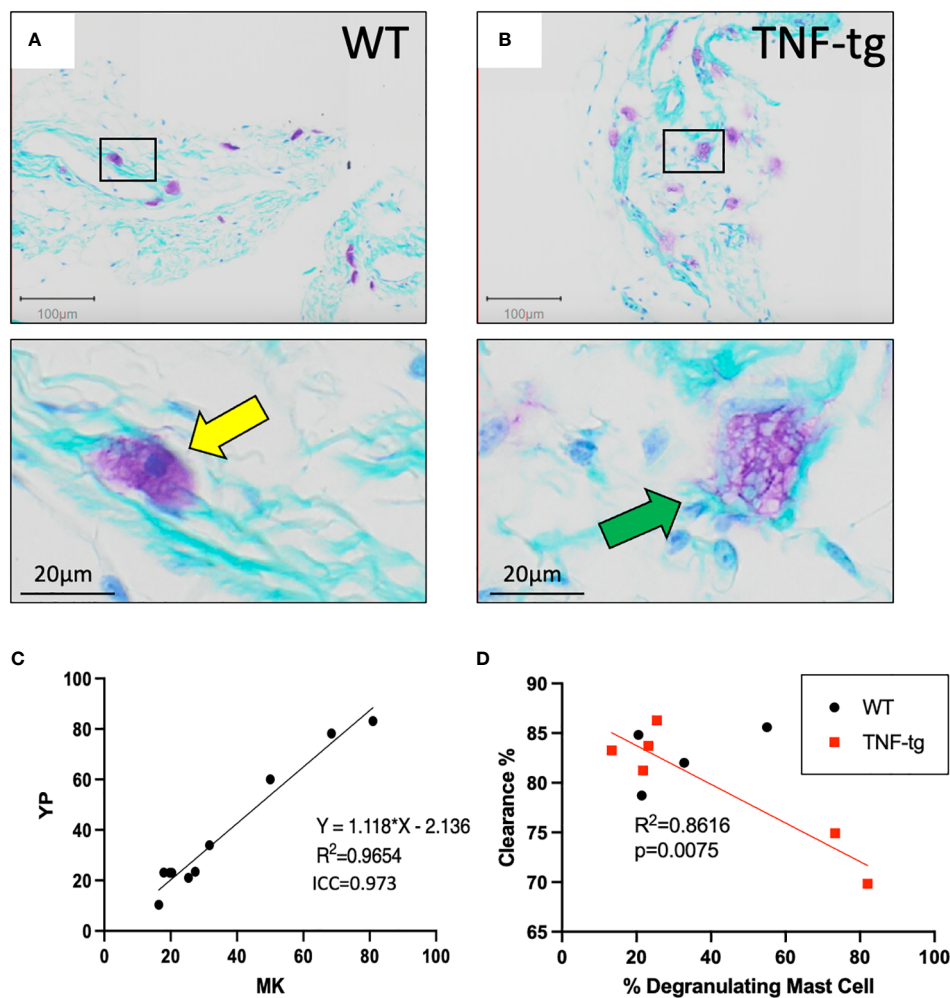


FIGURE 2

Degranulating peri-PLV mast cells are negatively associated with lymphatic function in WT and TNF-Tg mice. WT (A) and TNF-Tg (B) PLVs were processed for TBF-stained histology, and representative 5x images with corresponding 30x magnifications are shown to illustrate the non-degranulating mast cells (yellow arrow) with smaller and less obvious vacuoles in WT PLV, versus the degranulating mast cells with large granules (green arrow) associated with TNF-Tg PLV. (C) Histomorphometry by two observers (YP and MK) was performed to determine the ratio of degranulating: non-degranulating mast cells per PLV, and the data are presented as a linear regression with the slope, R^2 , and ICC values. (D) *In vivo* NIR-ICG imaging was performed on the lower limbs of WT and TNF-Tg mice to determine lymphatic clearance efficiency, and the imaged PLVs ($n=6$ for TNF-tg, $n=4$ for WT) were subsequently harvested to quantify the percentage of degranulating peri-PLV mast cells via histomorphometry of TBF-stained sections. The data are presented as simple linear regressions of ICG clearance % vs. % degranulating mast cells with p-value.

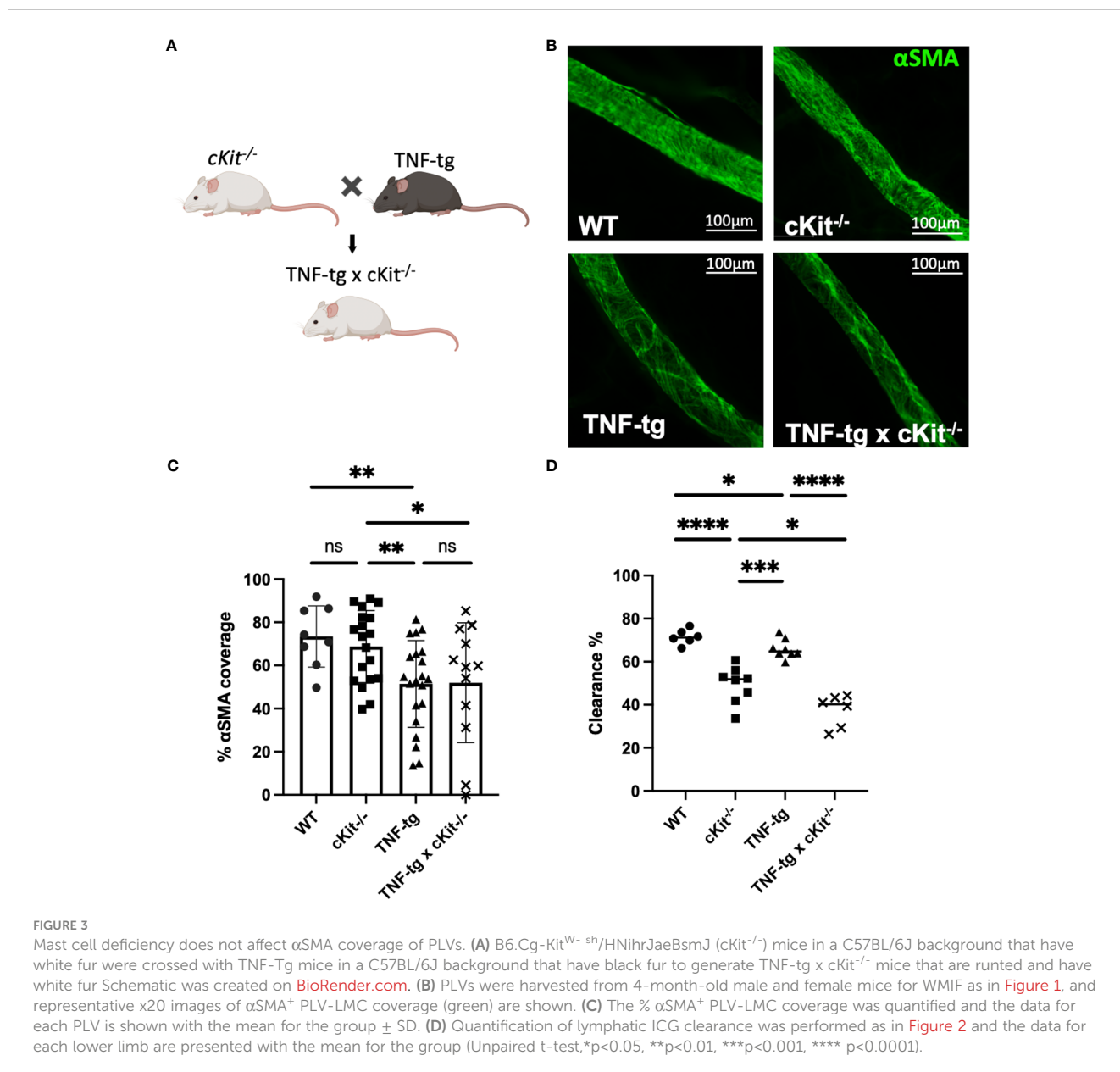
Mast cell deficiency ($cKit^{-/-}$) leads to reduced lymphatic function and exacerbation of inflammatory-erosive arthritis in TNF-tg mice

To assess the roles of mast cells in lymphatic homeostasis and inflammatory-erosive arthritis, we performed WMIFM, near-infrared indocyanine green imaging, micro-CT and histomorphometry on WT, $cKit^{-/-}$, TNF-tg and TNF-tg x $cKit^{-/-}$ mice (Figure 3A). The WMIFM results showed that α SMA⁺ LMC coverage of $cKit^{-/-}$ PLVs are similar to WT, in contrast to TNF-tg PLVs that are known to have decreased α SMA⁺ LMC coverage from chronic inflammation (4, 5). Moreover, mast cell deficiency did not further reduce α SMA⁺ LMC coverage of TNF-tg PLV (Figures 3B, C; $p=0.9511$). However, despite normal α SMA⁺ LMC coverage, $cKit^{-/-}$ PLVs displayed greater

functional defects in ICG clearance than TNF-tg PLVs, which presented as an additive functional deficiency in TNF-tg x $cKit^{-/-}$ mice (Figure 3D; $p<0.0001$). Taken together, these findings imply that the mechanism underlying reduced lymphatic clearance in $cKit^{-/-}$ mice is distinct from the loss of LMC structural proteins, and may in part be due to mast cell mediators known to influence lymphatic contractility (21, 23).

TNF-tg mice exhibit exacerbated bone erosion with mast cell deficiency

Micro-CT and histological analyses of ankle bones failed to identify any differences between WT and $cKit^{-/-}$ mice. The reduced bone volume, which is known to occur in TNF-tg mice (33, 34), is



attributed to both synovitis and osteoclastic resorption. Synovial inflammatory tissue expresses osteoclast differentiation factors and is the source of osteoclasts in RA (35, 36). Osteoclasts mediate bone resorption inside-out from the subchondral bone and outside-in from the periarticular surface (37). The severity of synovitis, evaluated by the synovial volume in H&E staining (Figures 4C, D; p= 0.0259), and osteoclastic resorption, indicated by TRAP staining (Figures 4C, E; p= 0.0089), were significantly exacerbated in TNF-tg x cKit^{-/-}, resulting in a greater reduction in bone volume compared to their TNF-tg littermates (Figures 4A, B; p= 0.0023).

Furthermore, mast cell deficiency was associated with reduced the overall health of TNF-tg mice as assessed by a significant decrease in body weight at ~4.5 month of age (Supplementary Figures 3A, B) and a significantly shortened life span (Supplementary Figure 3C) in both male and female TNF-tg x cKit^{-/-} mice.

Pharmacological inhibition of mast cell degranulation exacerbates lymphatic drainage and inflammatory-erosive arthritis in TNF-tg mice

As conclusions from our studies with TNF-tg x cKit^{-/-} mice are confounded by potential unaccounted defects during development and disruption of CD117/c-KIT and SCF/c-KIT signaling pathways in various organs (38), we aimed to corroborate our findings with pharmacological mast cell inhibition studies in adult TNF-tg mice with inflammatory-erosive arthritis. We selected cromolyn sodium (CS), an FDA-approved mast cell stabilizer that prevents release of inflammatory mediators such as histamine and leukotrienes, thereby inhibiting mast cell degranulation(39). In our study, two groups of 4-month-old female TNF-tg mice were treated with either CS or vehicle PBS for three weeks. The effectiveness of CS in

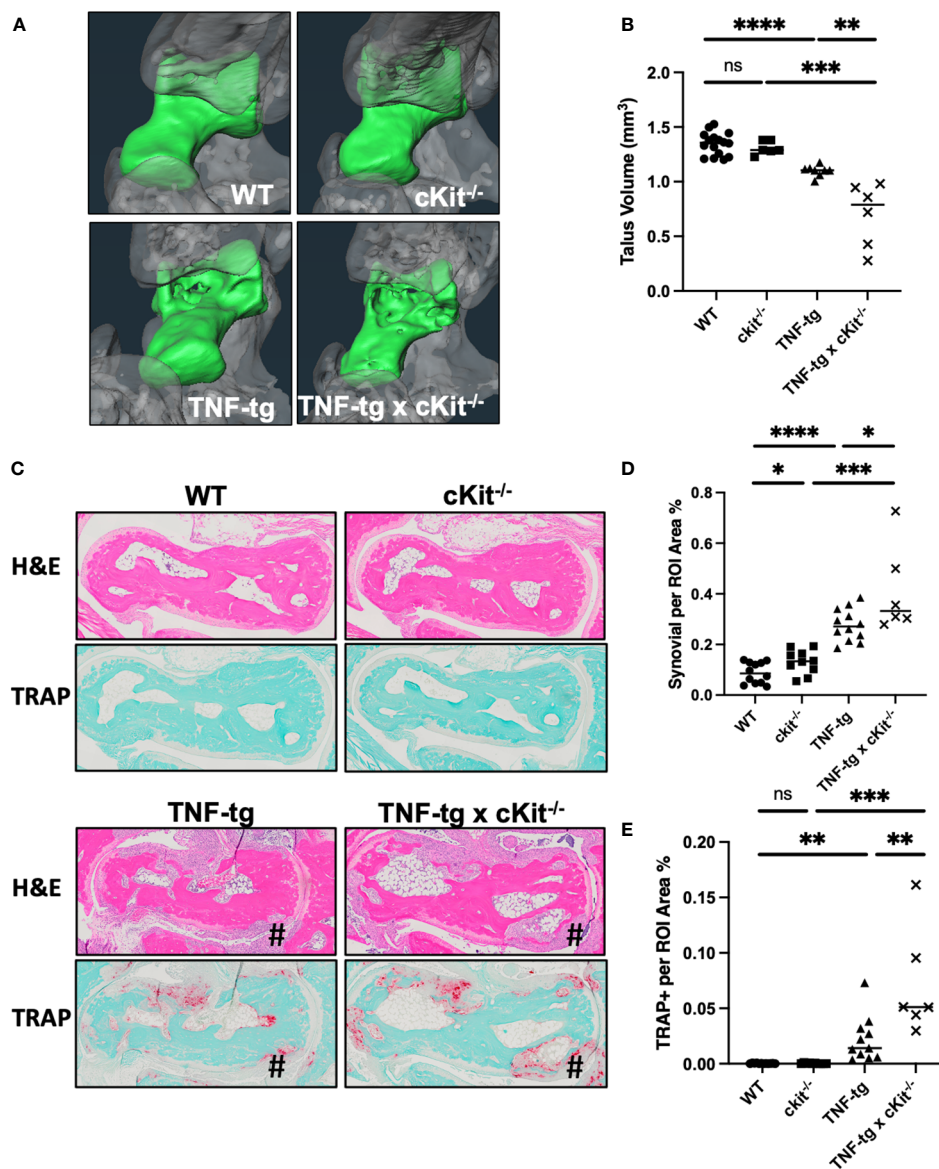


FIGURE 4 cKit deficiency exacerbates TNF-induced inflammatory-erosive arthritis in mice. **(A)** Micro-CT was performed on the ankles of the mice described in **Figure 3** and representative 3D renderings of the tali (green) are presented to illustrate the increased bone erosion in TNF-tg x cKit^{-/-} vs. TNF-tg mice. **(B)** Talus bone volume for each ankle are presented with the mean. **(C)** Representative H&E and TRAP-stained histology of the tali are shown at x4 to illustrate inflammation and osteoclasts at the site of bone erosion (#), with histomorphometry for synovitis **(D)** and osteoclasts **(E)**, and the data for each ankle (n ≥ 6) are presented with the mean (unpaired t test. *p<0.05, **p<0.01, ***p<0.001, ****p<0.0001).

inhibiting mast cell degranulation was confirmed by TBFG staining of PLV sections, which revealed a significantly decreased percentage of degranulating mast cells in the peri-PLV region after CS treatment, and markedly decreased overall health of TNF-tg mice (**Supplementary Figure 4**). Similar to cKit^{-/-} mice, our results showed that mice treated with CS exhibited reduced lymphatic clearance function compared to placebo controls (**Figures 5A, B**). Additionally, these mice showed increased bone erosion (**Figures 5C, D**) associated with more severe synovitis and osteoclast accumulation (**Figures 5E–G**).

These findings demonstrate the effectiveness of CS in inhibition of mast cell degranulation in the TNF-tg mouse model. Moreover, results from these pharmacology studies corroborate our genetic

findings demonstrate that mast cell activity (e.g. histamine release) is required for normal lymphatic function and that global inhibition of mast cells, either through genetic ablation or pharmacologic inhibition, exacerbates TNF-induced inflammatory-erosive arthritis in mice.

Identification of a distinct population of intra-lymphatic vessel mast cells

To better define the cellular subsets within and surrounding PLVs of WT and TNF-tg mice, we recently published a single-cell

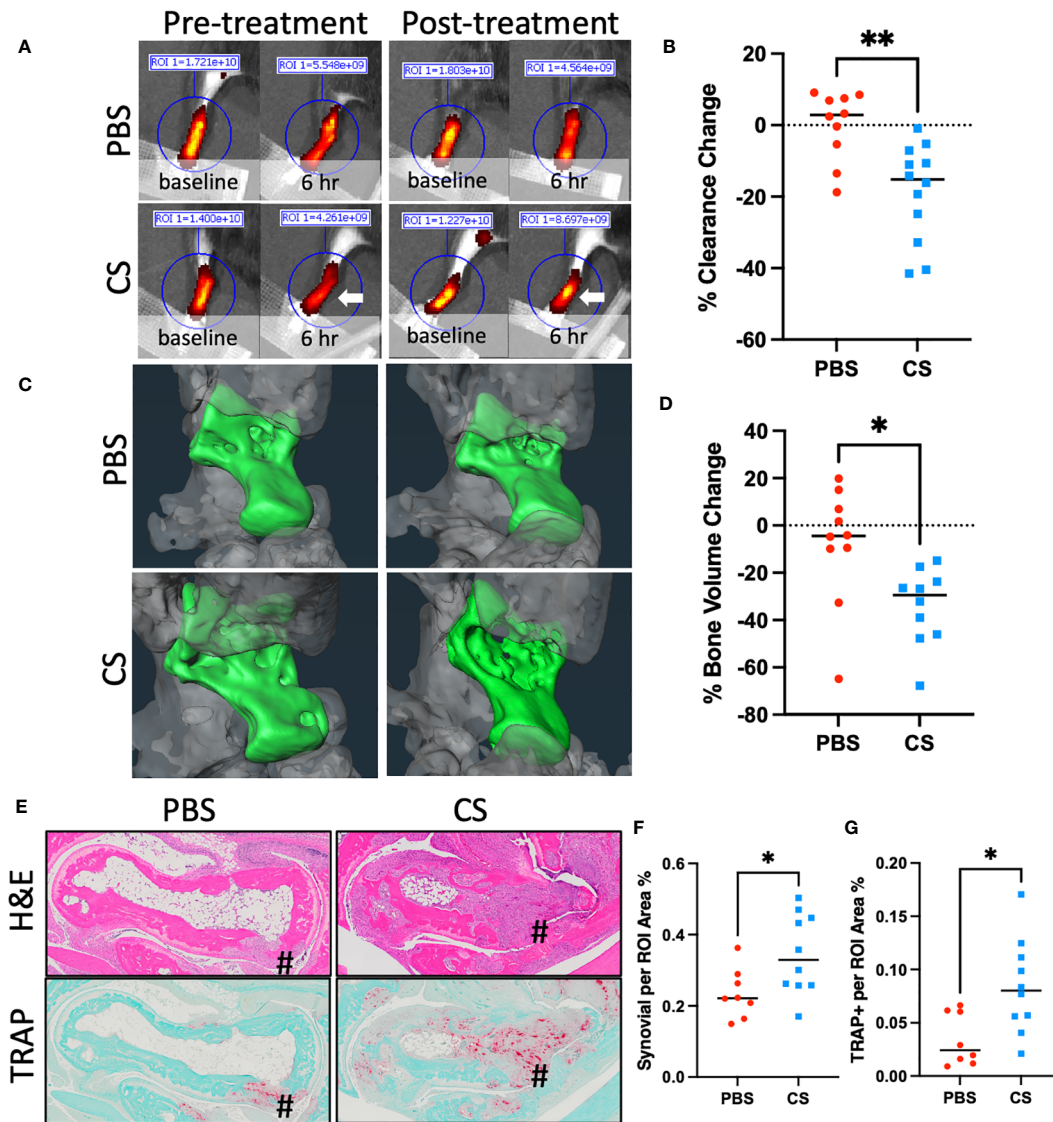


FIGURE 5 Cromolyn sodium treatment decreases lymphatic drainage and exacerbates inflammatory-erosive arthritis in TNF-Tg mice. 4-month-old female TNF-Tg mice (n = 5 animals; 10 lower limbs) were randomized to 3-weeks of placebo (PBS) or cromolyn sodium (CS), and longitudinal NIR-ICG imaging (A, B) and micro-CT (C, D) were performed to quantify lymphatic clearance and talus bone volume respectively. White arrow highlights the lack of clearance post-CS treatment. Post-treatment H&E and TRAP-stained histology are presented (E) with histomorphometry for synovitis (F) and osteoclasts (G) to illustrate exacerbated inflammatory-erosive arthritis (#) in CS treated TNF-Tg mice. Data for each lower limb (t-test, *p<0.05, **p<0.01).

RNA-sequencing (scRNAseq) study describing altered peri-PLV immune and stromal cells in inflammatory-erosive arthritis (28). Although these experiments were designed to primarily focus on LMCs, we obtained data on various hematopoietic cells including mast cells, although in small numbers as live peri-PLV mast cells are difficult to isolate following stringent dissection, tissue digestion, and cell washing steps used to isolated individual LMCs. To better understand these cells that are physically associated with PLVs and express mast cell marker genes (*Mcpt4*, *Cma1*, *Cpa3*, *Tpsb2*, *Kit*, *Fcer1a* & *Gata2*), we completed an *in silico* bioinformatic study that combined these data with datasets from a comprehensive UMAP of 242,000 cells encompassing various organs in the *Mouse Cell Atlas* (29). The extraction was performed based on the expression of the

mast cell marker genes, and following hierarchical re-clustering and integration, we derived a UMAP that revealed PLV mast cells that are phenotypically distinct from known mast cell populations in mice (Figure 6A). Interestingly, this cluster of PLV mast cells displayed increased TGF-beta signaling compared to other mast cell clusters via differential gene expression analysis (Figure 6B). To investigate the functional genomic implications of this discovery, we performed ENRICH Gene Ontology analysis on the genes exhibiting significantly increased expression in the PLV mast cell cluster. This analysis allowed us to identify pathways that may be upregulated in these PLV mast cells versus other mast cell clusters. The results from pathway analyses conducted using the WikiPathway 2021 human database and the Elsevier pathway

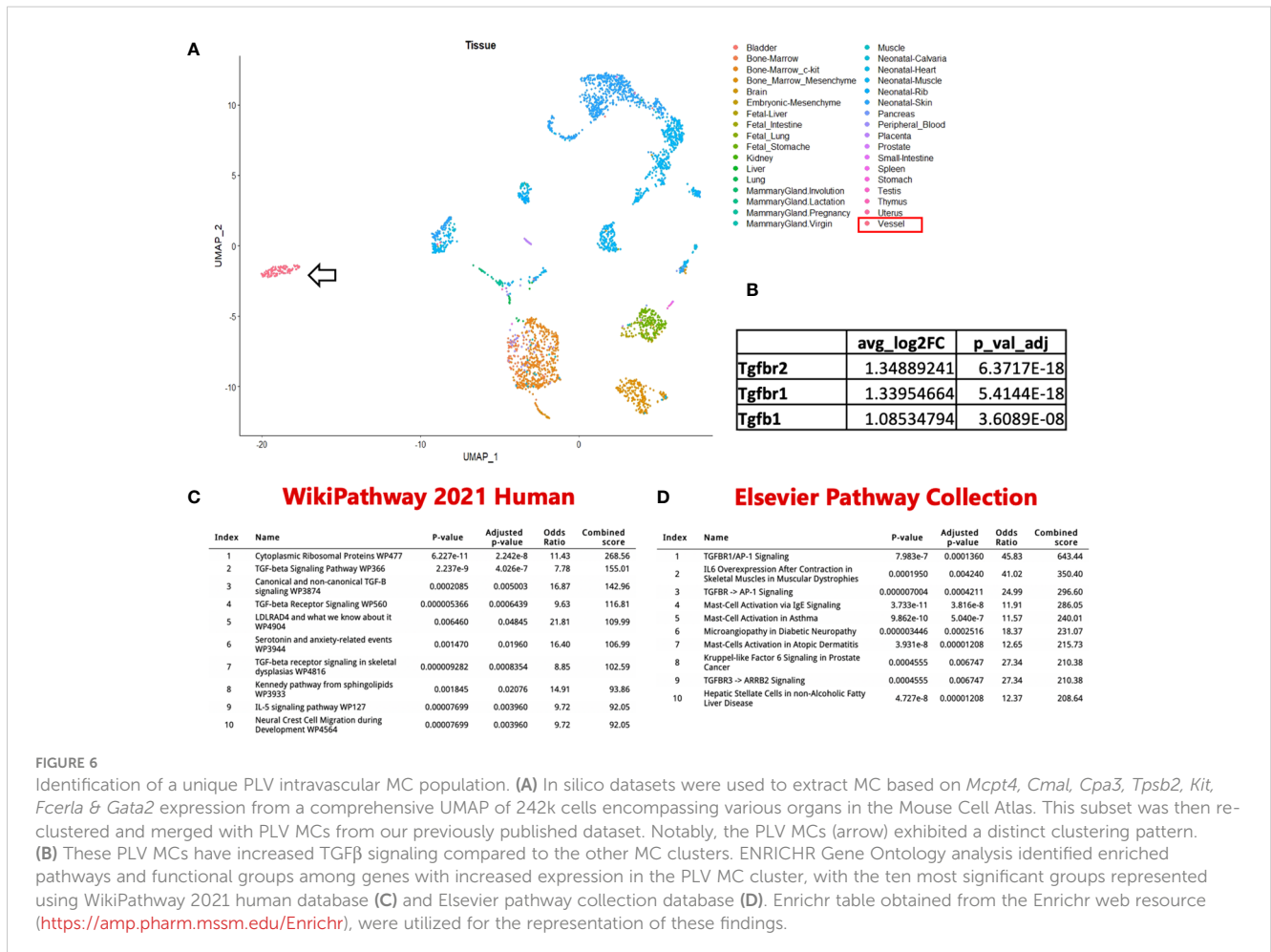
collection database are presented in **Figures 6C, D**, respectively. Notably, the PLV mast cell cluster displayed an elevated TGF-beta signaling pathway accompanied by increased mast cell activation, indicating potential anti-inflammatory and anabolic functions. While this preliminary *in silico* finding of increased TGF-beta signaling in WT peri-PLV mast cells is provocative, it is possible that signaling pathways in homeostatic mast cells are different from peri-PLV mast cells in TNF-tg mice with inflammatory arthritis. Thus, TGF-beta signaling might not fully explain the contribution of mast cells in this model.

An unexplained finding in our prior α SMA WMIFM studies in lineage tracing and PLV repair experiments is the frequently observed presence of rounded cell-shape-like empty spaces within PLVs that lacked α SMA staining (4, 26, 40). Based on our *in silico* data predicting that a unique PLV-associated mast cell population exists, we re-examined our PLV histology and discovered purple toluidine blue stained cells buried within the lymphatic vessel wall (**Figure 7A**), located between the layers of lymphatic endothelial cells and LMCs. Given the similar size of these cells to the empty spaces in our α SMA WMIFM images, which we have repeatedly observed in our prior studies (4, 26, 40), we hypothesized that these “voids” might be occupied by a distinct population of intra-PLV mast cells. To test this, PLVs were subjected to WMIFM for α SMA and MCT, and we found that the gaps between the α SMA⁺ LMC contained cells with similar

positive staining for MCT as the peri-PLV mast cells (**Figure 7B**), confirming the presence of intravascular mast cells within PLV. To further characterize these peri- and intra-PLV mast cells, we performed WMIFM with antibodies specific from mast cell proteases (MCPT1, 4 & 5). The results demonstrated that peri-PLV mast cells are MCPT1⁺ MCPT4⁺ while intra-PLV mast cells are MCPT1⁻ MCPT4⁻ (**Figures 7C, D**), further confirming that these are distinct populations of mast cells. Despite our prediction that these mast cells expressed MCPT5 from the scRNAseq data (**Supplementary Table 1**), our WMIFM studies failed to detect any positive staining in or around PLVs (**Figures 7E**).

Discussion

Mast cells modulate the course of inflammatory arthritis through recruitment and activation of synovial macrophages (13), which produce the bulk of the pro-inflammatory cytokines in the RA joint, most notably TNF and IL-1. Of note is that mast cells also release these pro-inflammatory cytokines in inflammatory arthritis following JNK1-mediated mast cell degranulation (41). Additionally, clinical studies have shown that mast cells in early RA are associated with disease severity, and support B cell autoantibody production (18, 42).



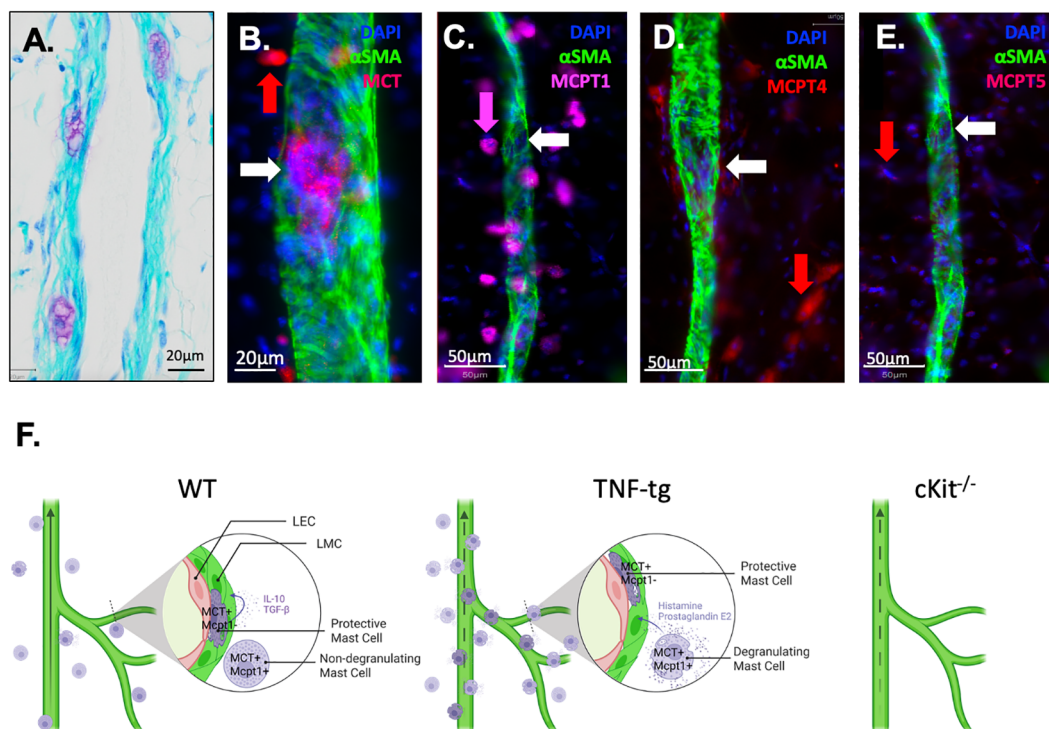


FIGURE 7

Phenotypic distinction between peri-PLV mast cells versus intravascular mast cells and proposed model of their pro and anti-inflammatory functions. (A) A 20x micrograph of a TBFStained WT PLV is shown to highlight the novel intravascular MC identified in this study, which is embedded within the PLV wall, situated between the layers of lymphatic endothelial cells and lymphatic muscle cells. WMIFM was performed on TNF-tg PLV for α SMA and MCT, MCPT1, MCPT4 and MCPT5 as described in Figure 1. (B) 40x image highlighting MCT⁺ perivascular MC (red arrow) and MCT1⁺ intravascular MC (white arrow). (C) 20x image highlighting MCPT1⁺ perivascular MC (pink arrow) and MCPT1⁻ intravascular MC (white arrow). (D) 20x image highlighting MCPT4⁺ perivascular MC (red arrow) and MCPT4⁻ intravascular MC (white arrow). (E) 20x image highlighting MCPT5⁺ perivascular MC (red arrow) and MCPT5⁻ intravascular MC (white arrow). (F) Schematic illustration of MCT⁺/MCPT1⁺ conventional pro-inflammatory peri-lymphatic vessel mast cells and a novel homeostatic MCT⁺/MCPT1⁻ intra-lymphatic vessel mast cell population. Schematic was created on [biorender.com](https://www.biorender.com).

Mast cells have also been studied in animal models of RA for over 50 years (43), and the results have varied based on the particular murine model used and experimental approaches. Some studies showed that mast cell depletion in the preclinical phase of collagen-induced arthritis (CIA) reduces the clinical outcome by lowering the inflammatory cytokine profile (44), while others demonstrated that CIA is not impaired in mast cell-deficient mice (45). In contrast, studies in the K/BxN serum-induced arthritis model showed that both W/Wv and Sl/Sld mast cell deficient mice are resistant to development of joint inflammation. Sl/Sld mice are only capable of encoding a soluble truncated cKit ligand that lacks both transmembrane and cytoplasmic domains(46, 47), while cKit ligand in W/Wv mice lacks kinase activity and is not expressed on the cell surface(48). Bone marrow mast cell engraftment restores susceptibility to arthritis in W/Wv mice, confirming that the resistance to arthritis induced by K/BxN serum transfer was due to the absence of mast cells in the mutant mice, and not to defects in other cell types (49).

Interestingly, Schubert et al. found a redundant role of mast cells in the K/BxN model, where joint inflammation was triggered by cartilage-bound immune complexes independently of T cells, while mast cells were critical for T-cell dependent CIA (50). Collectively, these studies suggest that mast cells may function as a cellular link between soluble mediators, autoantibodies, and other

effector cells (i.e., T cells and osteoclasts), but appear to be dispensable for antibody-induced arthritis.

While the aforementioned work was largely focused on mast cells in the RA joint and animal models of acute inflammatory-erosive arthritis, our research interests have been centered on questions of arthritic flare in the setting of long-standing RA and progressive joint disease in chronic models. This unbiased research uncovered several parallel changes that occur in joint draining lymphatic vessels and lymph nodes of RA patients and TNF-tg mice, and have been broadly characterized by an initial “expansion” phase of mild disease with lymphangiogenesis and enlargement of efferent lymph nodes, followed by loss of efferent lymphatics, “collapse” of the joint draining lymph nodes and exacerbated synovitis and joint erosion at end-stage disease (8, 51). As the lymphatic deficits during the collapse phase are intrinsic to the lymphatic vessels themselves (3, 5), we completed a scRNAseq analysis of PLV from TNF-tg mice with inflammatory-erosive arthritis vs. WT controls (28). While this study confirmed our hypothesis of lymphatic muscle cell and M2 macrophage loss with a commensurate increase in inflammatory monocytes in TNF-tg lymphatic vessels, we also observed a surprising 3.6-fold decrease in the number TNF-tg mast cells, in addition to other hematopoietic cells that may also affect lymphatic function. This observation also appears to be inconsistent with our finding of a 2.6-fold

increase in peri-PLV mast cells in TNF-tg vs. WT observed using WMIFM for MCT (Figure 1). However, it is important to note that the stringent PLV dissection, enzymatic digestion, and single-cell isolation procedures used for scRNAseq would be expected to eliminate the loosely adherent and unstable-degranulating mast cells observed in Figure 1 from the analysis. Thus, we interpret this loss of mast cells in TNF-tg PLV to be a specific decrease in the novel intravascular mast cells which exist stably embedded within vessel walls that we identified in this study (Figures 7A, B).

Based on the literature and our novel findings, we conclude that subpopulations of mast cells exist in and around lymphatic vessels (Figure 7). During homeostasis, the peri-lymphatic MC are dormant in their non-degranulating form, while the intravascular MC release anti-inflammatory and anabolic factors that sustain lymphatic vessel structure and function. Thus, global loss of intravascular MC in *cKit*^{-/-} results in loss of lymphatic drainage. Chronic inflammatory arthritis stimulates accumulation and degranulation of peri-vascular MC, which produce pro-inflammatory and catabolic factors that overwhelm intravascular MC to permeabilize and degenerate lymphatic vessels. As other cells also produce these factors during chronic inflammation, loss of all MC including the intravascular MC in *cKit*^{-/-} and cromolyn sodium treatment has a net result of exacerbated synovitis and erosive arthritis (Figure 7F).

We hypothesize that the TNF-induced peri-PLV mast cells are of the canonical pro-inflammatory subtype, while the mast cells embedded within the vessel are of a homeostatic/anti-inflammatory subtype that has a protective role during inflammatory arthritis. Our *in silico* data demonstrating potential TGF-beta signaling in these intra-PLV mast cells suggest that they may be akin to mast cells involved in wound healing (52). It is also interesting that these PLV-associated mast cell populations are phenotypically distinct based on MCPT1 and MCPT4 expression (Figure 7C), which opens possibilities for selective-inducible depletion of a specific mast cell population with genetic models. It might also be possible to isolate mast in the presence of mast stabilizers, and assess functional characteristics between WT vs TNF-tg mast cells *in vitro*.

Several noteworthy limitations to our study deserve mention. Most notable is that our experimental approach to assess MC loss of function (*cKit*^{-/-} and CS treated mice) affects all MC systemically, such that specific conclusions of the distinct roles of peri-PLV and intra-PLV MC cannot be made at this time. Nonetheless, our hypothesis generating findings support our speculation that intravascular mast cells play a homeostatic/protective role in lymphatic function and joint preservation is based on the simplest explanation of the observed defective ICG clearance in *cKit*^{-/-} and CS treated mice, and exacerbated inflammatory-erosive arthritis in mast cell deficient TNF-tg mice, and warrants future studies to confirm this with direct evidence. Additional support for this speculation also came from functional genomic data demonstrating increased TGF-beta signaling in intravascular mast cells compared to other mast cell subtypes. However, our attempts to confirm this via WMIFM of TGF-beta and TGF-beta receptors failed to produce credible data, and efforts to improve our methods are ongoing.

Another limitation relates to the *Kit*^{W-sh/W-sh} mouse model, which exhibits mast cell deficiency and maintains normal levels of

differentiated hematopoietic and lymphoid cells without anemia or sterility, making it a suitable choice for our study considering its favorable characteristics compared to *Kit*^{W/W-v} mice. However, *Kit*^{W-sh/W-sh} mice still display c-Kit tyrosine kinase-dependent signaling related abnormalities, lack interstitial cells of Cajal in the gut, and exhibited bile reflux into the stomach. Although it is unlikely that these defects contribute to the specific PLV and ankle arthritis phenotypes we observed, we acknowledge these confounders in our data analyses, and the importance of investigating mast cell subtypes and selectively inhibiting or deleting inflammatory mast cells. Based on our finding of differential expression of MCPT1 and MCPT4 in peri vs. intravascular mast cells, this should be possible using a genetic approach that utilizes *Mcpt1*-target or *Mcpt4*-target gene expression akin to *Mcpt1*-Cre-iDTR mice (53). Our future research will focus on generating MC-subpopulation-specific mast cell strains, such as the *Mcpt1* DTR murine model, which would enable selective *in vivo* depletion of *Mcpt1*-expressing mast cells (54). Alternatively, it might be possible to generate a depletion model with CRISPR to selectively remove the identified mast cell subpopulations *in vitro* in the presence of mast cell stabilizer.

Our *in silico* analysis revealed the expression of *Mcpt5*, which is a mast cell chymase typically found in connective tissue mast cells (55). However, despite our efforts, we were unable to detect any *Mcpt5*⁺ mast cells via WMIFM. This could be attributed to post-transcriptional regulation of *Mcpt5* or potential issues with the antibodies used in our study. Thus, future studies are needed to sort this out.

In summary, we demonstrate that two distinct populations of mast cells exist in and around joint draining PLV. The peri-PLV mast cell population expands in the setting of chronic TNF-induced inflammatory-erosive arthritis, and likely contributes to lymphatic dysfunction as their degranulated fraction is inversely correlated with ICG clearance. However, as genetic depletion and pharmacologic inhibition of mast cells exacerbates inflammatory-erosive arthritis and lymphatic dysfunction without damaging LMCs, we infer that intra-PLV mast cells may produce critical signals for LMC contraction and efficient lymph flow, and future studies to test this are warranted. Additionally, as prior mast cell loss of function studies in arthritis models have focused on direct effects within the joint, interpretation of these results may benefit from consideration of the mast cell indirect effects on arthritis via their regulation of lymphatic function.

Data availability statement

The datasets presented in this study can be found in online repositories. The names of the repository/repositories and accession number(s) can be found in the article/Supplementary Material.

Ethics statement

The animal study was approved by University of Rochester Committee for Animal Resources. The study was conducted in accordance with the local legislation and institutional requirements.

Author contributions

YP: Writing – original draft, Writing – review & editing. HK: Writing – review & editing. KB: Writing – review & editing. LX: Writing – review & editing. CR: Writing – review & editing. ES: Funding acquisition, Project administration, Supervision, Writing – review & editing.

Funding

The author(s) declare financial support was received for the research, authorship, and/or publication of this article. This work was supported by funding from the National Institutes of Health: T32 GM007356 (HK), T32 AR076950 (HK), R01 AG059775 (LX), R01 AR069000 (CR), R01 AR056702 (ES), P30 AR069655 (ES), and F30 AG076326 (HK).

Acknowledgments

We would like to thank the faculty and staff at the Genomics Research Center and Histology, Biochemistry, the Electron Microscopy Resource in the Center for Advanced Resource Technologies, and Molecular Imaging Core at the University of Rochester Medical Center.

References

1. Gravallese EM, Firestein GS. Rheumatoid arthritis - common origins, divergent mechanisms. *N Engl J Med* (2023) 388:529–42. doi: 10.1056/NEJMra2103726
2. Bell RD, Rahimi H, Kenney HM, Lieberman AA, Wood RW, Schwarz EM, et al. Altered lymphatic vessel anatomy and markedly diminished lymph clearance in affected hands of patients with active rheumatoid arthritis. *Arthritis Rheumatol* (2020) 72:1447–55. doi: 10.1002/art.41311
3. Scallan JP, Bouta EM, Rahimi H, Kenney HM, Ritchlin CT, Davis MJ, et al. Ex vivo demonstration of functional deficiencies in popliteal lymphatic vessels from TNF-transgenic mice with inflammatory arthritis. *Front Physiol* (2021) 12:745096. doi: 10.3389/fphys.2021.745096
4. Kenney HM, Peng Y, Bell RD, Wood RW, Xing L, Ritchlin CT, et al. Persistent popliteal lymphatic muscle cell coverage defects despite amelioration of arthritis and recovery of popliteal lymphatic vessel function in TNF-Tg mice following anti-TNF therapy. *Sci Rep* (2022) 12:12751. doi: 10.1038/s41598-022-16884-y
5. Bouta EM, Kuzin I, De Mesy Bentley K, Wood RW, Rahimi H, Ji RC, et al. Brief report: treatment of tumor necrosis factor-transgenic mice with anti-tumor necrosis factor restores lymphatic contractions, repairs lymphatic vessels, and may increase monocyte/macrophage egress. *Arthritis Rheumatol* (2017) 69:1187–93. doi: 10.1002/art.40047
6. Li J, Kuzin I, Moshkani S, Proulx ST, Xing L, Skrombolas D, et al. Expanded CD23 (+)/CD21 (hi) B cells in inflamed lymph nodes are associated with the onset of inflammatory-erosive arthritis in TNF-transgenic mice and are targets of anti-CD20 therapy. *J Immunol* (2010) 184:6142–50. doi: 10.4049/jimmunol.0903489
7. Li J, Ju Y, Bouta EM, Xing L, Wood RW, Kuzin I, et al. Efficacy of B cell depletion therapy for murine joint arthritis flare is associated with increased lymphatic flow. *Arthritis Rheum* (2012) 65:130–8. doi: 10.1002/art.37709
8. Bouta EM, Bell RD, Rahimi H, Xing L, Wood RW, Bingham CO 3rd, et al. Targeting lymphatic function as a novel therapeutic intervention for rheumatoid arthritis. *Nat Rev Rheumatol* (2018) 14:94–106. doi: 10.1038/nrrheum.2017.205
9. Bell RD, Slattery PN, Wu EK, Xing L, Ritchlin CT, Schwarz EM. iNOS dependent and independent phases of lymph node expansion in mice with TNF-induced inflammatory-erosive arthritis. *Arthritis Res Ther* (2019) 21:240. doi: 10.1186/s13075-019-2039-z
10. Bromley M, Fisher WD, Woolley DE. Mast cells at sites of cartilage erosion in the rheumatoid joint. *Ann Rheum Dis* (1984) 43:76–9. doi: 10.1136/ard.43.1.76

Conflict of interest

The authors declare that the research was conducted in the absence of any commercial or financial relationships that could be construed as a potential conflict of interest.

Publisher's note

All claims expressed in this article are solely those of the authors and do not necessarily represent those of their affiliated organizations, or those of the publisher, the editors and the reviewers. Any product that may be evaluated in this article, or claim that may be made by its manufacturer, is not guaranteed or endorsed by the publisher.

Supplementary material

The Supplementary Material for this article can be found online at: <https://www.frontiersin.org/articles/10.3389/fimmu.2023.1275871/full#supplementary-material>

11. Godfrey HP, Ilardi C, Engber W, Graziano FM. Quantitation of human synovial mast cells in rheumatoid arthritis and other rheumatic diseases. *Arthritis Rheum* (1984) 27:852–6. doi: 10.1002/art.1780270803
12. Malone DG, Wilder RL, Saavedra-Delgado AM, Metcalfe DD. Mast cell numbers in rheumatoid synovial tissues. Correlations with quantitative measures of lymphocytic infiltration and modulation by antiinflammatory therapy. *Arthritis Rheum* (1987) 30:130–7. doi: 10.1002/art.1780300202
13. Nigrovic PA, Lee DM. Mast cells in inflammatory arthritis. *Arthritis Res Ther* (2004) 7:1. doi: 10.1186/ar1446
14. Solimando AG, Desantis V, Ribatti D. Mast cells and interleukins. *Int J Mol Sci* (2022) 23:8. doi: 10.3390/ijms232214004
15. Gutowski L, Kanikowski S, Formanowicz D. Mast cell involvement in the pathogenesis of selected musculoskeletal diseases. *Life (Basel)* (2023) 13:3. doi: 10.3390/life13081690
16. Wilgus TA, Ud-Din S, Bayat A. A review of the evidence for and against a role for mast cells in cutaneous scarring and fibrosis. *Int J Mol Sci* (2020) 21(24):9673. doi: 10.3390/ijms21249673
17. Chang MH, Levescot A, Nelson-Maney N, Blaustein RB, Winden KD, Morris A, et al. Arthritis flares mediated by tissue-resident memory T cells in the joint. *Cell Rep* (2021) 37:109902. doi: 10.1016/j.celrep.2021.109902
18. Rivellesse F, Mauro D, Nerviani A, Pagani S, Fossati-Jimack L, Messemaker T, et al. Mast cells in early rheumatoid arthritis associate with disease severity and support B cell autoantibody production. *Ann Rheum Dis* (2018) 77:1773–81. doi: 10.1136/annrheumdis-2018-213418
19. Nigrovic PA, Lee DM. Mast cells in inflammatory arthritis. *Arthritis Res Ther* (2005) 7:1–11. doi: 10.1186/ar1446
20. Krystel-Whittemore M, Dileepan KN, Wood JG. Mast cell: A multi-functional master cell. *Front Immunol* (2015) 6:620. doi: 10.3389/fimmu.2015.00620
21. Plaku KJ, Von Der Weid PY. Mast cell degranulation alters lymphatic contractile activity through action of histamine. *Microcirculation* (2006) 13:219–27. doi: 10.1080/10739680600556902
22. Scallan JP, Davis MJ. Itching for answers: how histamine relaxes lymphatic vessels. *Microcirculation* (2014) 21:575–7. doi: 10.1111/micc.12162

23. Pal S, Nath S, Meininger CJ, Gashev AA. Emerging roles of mast cells in the regulation of lymphatic immuno-physiology. *Front Immunol* (2020) 11:1234. doi: 10.3389/fimmu.2020.01234
24. Fox JL, Von Der Weid PY. Effects of histamine on the contractile and electrical activity in isolated lymphatic vessels of the Guinea-pig mesentery. *Br J Pharmacol* (2002) 136:1210–8. doi: 10.1038/sj.bjp.0704820
25. Keffer J, Probert L, Cazlaris H, Georgopoulos S, Kaslaris E, Kioussis D, et al. Transgenic mice expressing human tumour necrosis factor: a predictive genetic model of arthritis. *EMBO J* (1991) 10:4025–31. doi: 10.1002/j.1460-2075.1991.tb04978.x
26. Kenney HM, Bell RD, Masters EA, Xing L, Ritchlin CT, Schwarz EM. Lineage tracing reveals evidence of a popliteal lymphatic muscle progenitor cell that is distinct from skeletal and vascular muscle progenitors. *Sci Rep* (2020) 10:18088. doi: 10.1038/s41598-020-75190-7
27. Hori Y, Takeda S, Cho H, Wegmann S, Shoup TM, Takahashi K, et al. and Drug Administration-approved asthma therapeutic agent impacts amyloid β in the brain in a transgenic model of Alzheimer disease. *J Biol Chem* (2015) 290:1966–78. doi: 10.1074/jbc.M114.586602
28. Kenney HM, Wu CL, Loissele AE, Xing L, Ritchlin CT, Schwarz EM. Single-cell transcriptomics of popliteal lymphatic vessels and peripheral veins reveals altered lymphatic muscle and immune cell populations in the TNF-Tg arthritis model. *Arthritis Res Ther* (2022) 24:64. doi: 10.1186/s13075-022-02730-z
29. Han X, Wang R, Zhou Y, Fei L, Sun H, Lai S, et al. Mapping the mouse cell atlas by microwell-seq. *Cell* (2018) 173:1307. doi: 10.1016/j.cell.2018.05.012
30. Fei L, Chen H, Ma L, Weigao E, Wang R, Fang X, et al. Systematic identification of cell-fate regulatory programs using a single-cell atlas of mouse development. *Nat Genet* (2022) 54:1051–61. doi: 10.1038/s41588-022-01118-8
31. Wang R, Zhang P, Wang J, Ma L, Weigao E, Suo S, et al. Construction of a cross-species cell landscape at single-cell level. *Nucleic Acids Res* (2022) 51:501–16. doi: 10.1093/nar/gkac633
32. Sridharan G, Shankar AA. Toluidine blue: A review of its chemistry and clinical utility. *J Oral Maxillofac Pathol* (2012) 16:251–5. doi: 10.4103/0973-029X.99081
33. Kenney HM, Peng Y, Chen KL, Ajalik R, Schnur L, Wood RW, et al. A high-throughput semi-automated bone segmentation workflow for murine hindpaw micro-CT datasets. *Bone Rep* (2022) 16:101167. doi: 10.1016/j.bonr.2022.101167
34. Kenney HM, Wood RW, Ramirez G, Bell RD, Chen KL, Schnur L, et al. Implementation of automated behavior metrics to evaluate voluntary wheel running effects on inflammatory-erosive arthritis and interstitial lung disease in TNF-Tg mice. *Arthritis Res Ther* (2023) 25:17. doi: 10.1186/s13075-022-02985-6
35. Gravalles EM, Manning C, Tsay A, Naito A, Pan C, Amento E, et al. Synovial tissue in rheumatoid arthritis is a source of osteoclast differentiation factor. *Arthritis Rheum* (2000) 43:250–8. doi: 10.1002/1529-0131(200002)43:2<250::AID-ANR3>3.0.CO;2-P
36. Schett G. Cells of the synovium in rheumatoid arthritis. Osteoclasts. *Arthritis Res Ther* (2007) 9:203. doi: 10.1186/ar2110
37. Löfvall H, Newbould H, Karsdal MA, Dziegiel MH, Richter J, Henriksen K, et al. Osteoclasts degrade bone and cartilage knee joint compartments through different resorption processes. *Arthritis Res Ther* (2018) 20:67. doi: 10.1186/s13075-018-1564-5
38. Grimaldeston MA, Chen CC, Piliponsky AM, Tsai M, Tam SY, Galli SJ. Mast cell-deficient W-sash c-kit mutant Kit W-sh/W-sh mice as a model for investigating mast cell biology in vivo. *Am J Pathol* (2005) 167:835–48. doi: 10.1016/S0002-9440(10)62055-X
39. Kunder CA, St John AL, Abraham SN. Mast cell modulation of the vascular and lymphatic endothelium. *Blood* (2011) 118:5383–93. doi: 10.1182/blood-2011-07-358432
40. Kenney HM, Peng Y, De Mesy Bentley KL, Xing L, Ritchlin CT, Schwarz EM. The enigmas of lymphatic muscle cells: where do they come from, how are they maintained, and can they regenerate? *Curr Rheumatol Rev* (2023) 19:246–59. doi: 10.2174/1573397119666230127144711
41. Guma M, Kashiwakura J, Crain B, Kawakami Y, Beutler B, Firestein GS, et al. JNK1 controls mast cell degranulation and IL-1 β production in inflammatory arthritis. *Proc Natl Acad Sci U.S.A.* (2010) 107:22122–7. doi: 10.1073/pnas.1016401107
42. Rivellesse F, Rossi FW, Giorli G, Napolitano F, De Paulis A, Pitzalis C. Persistence of mast cell-positive synovitis in early rheumatoid arthritis following treatment with conventional synthetic disease modifying anti-rheumatic drugs. *Front Pharmacol* (2020) 11:1051. doi: 10.3389/fphar.2020.01051
43. Gryfe A, Sanders PM, Gardner DL. The mast cell in early rat adjuvant arthritis. *Ann Rheum Dis* (1971) 30:24–30. doi: 10.1136/ard.30.1.24
44. Van Der Velden D, Lagraauw HM, Wezel A, Launay P, Kuiper J, Huizinga TW, et al. Mast cell depletion in the preclinical phase of collagen-induced arthritis reduces clinical outcome by lowering the inflammatory cytokine profile. *Arthritis Res Ther* (2016) 18:138. doi: 10.1186/s13075-016-1036-8
45. Pitman N, Asquith DL, Murphy G, Liew FY, McInnes IB. Collagen-induced arthritis is not impaired in mast cell-deficient mice. *Ann Rheum Dis* (2011) 70:1170–1. doi: 10.1136/ard.2010.134528
46. Zsebo KM, Williams DA, Geissler EN, Broudy VC, Martin FH, Atkins HL, et al. Stem cell factor is encoded at the Sl locus of the mouse and is the ligand for the c-kit tyrosine kinase receptor. *Cell* (1990) 63:213–24. doi: 10.1016/0092-8674(90)90302-U
47. Brannan CI, Lyman SD, Williams DE, Eisenman J, Anderson DM, Cosman D, et al. Steel-Dickie mutation encodes a c-kit ligand lacking transmembrane and cytoplasmic domains. *Proc Natl Acad Sci U.S.A.* (1991) 88:4671–4. doi: 10.1073/pnas.88.11.4671
48. Nocka K, Tan JC, Chiu E, Chu TY, Ray P, Traktman P, et al. Molecular bases of dominant negative and loss of function mutations at the murine c-kit/white spotting locus: W37, Wv, W41 and W. *EMBO J* (1990) 9:1805–13. doi: 10.1002/j.1460-2075.1990.tb08305.x
49. Lee DM, Friend DS, Gurish MF, Benoist C, Mathis D, Brenner MB. Mast cells: a cellular link between autoantibodies and inflammatory arthritis. *Science* (2002) 297:1689–92. doi: 10.1126/science.1073176
50. Schubert N, Dudeck J, Liu P, Karutz A, Speier S, Maurer M, et al. Mast cell promotion of T cell-driven antigen-induced arthritis despite being dispensable for antibody-induced arthritis in which T cells are bypassed. *Arthritis Rheumatol* (2015) 67:903–13. doi: 10.1002/art.38996
51. Bouta EM, Li J, Ju Y, Brown EB, Ritchlin CT, Xing L, et al. The role of the lymphatic system in inflammatory-erosive arthritis. *Semin Cell Dev Biol* (2015) 38:90–7. doi: 10.1016/j.semcdb.2015.01.001
52. Bacci S. Fine regulation during wound healing by mast cells, a physiological role not yet clarified. *Int J Mol Sci* (2022) 23:6–7. doi: 10.3390/ijms23031820
53. Zhang L, Wang T, Chang M, Kaiser C, Kim JD, Wu T, et al. Teriparatide treatment improves bone defect healing via anabolic effects on new bone formation and non-anabolic effects on inhibition of mast cells in a murine cranial window model. *J Bone Miner Res* (2017) 32:1870–83. doi: 10.1002/jbmr.3178
54. Sasaki H, Imanishi M, Fujikura D, Sugiyama M, Tanimoto K, Mochiji Y, et al. New inducible mast cell-deficient mouse model (Mcp5/Cma1DTR). *Biochem Biophys Res Commun* (2021) 551:127–32. doi: 10.1016/j.bbrc.2021.03.025
55. Nagata K, Nishiyama C. IL-10 in mast cell-mediated immune responses: anti-inflammatory and proinflammatory roles. *Int J Mol Sci* (2021) 22:4. doi: 10.3390/ijms22094972